

Osteoarthritis and Cartilage



Intra-articular basic calcium phosphate and monosodium urate crystals inhibit anti-osteoclastogenic cytokine signalling



C.C. Cunningham †‡, E.M. Corr †‡, G.M. McCarthy §, A. Dunne †‡*

† School of Biochemistry & Immunology, Trinity Biomedical Sciences Institute, Trinity College Dublin, Ireland

‡ School of Medicine, Trinity Biomedical Sciences Institute, Trinity College Dublin, Ireland

§ Mater Misericordiae University Hospital, Dublin 7, Ireland

ARTICLE INFO

Article history:

Received 14 January 2016

Accepted 1 July 2016

Keywords:

Osteoclasts

Crystal deposition disease

Osteoarthritis

Gout

SUMMARY

Objective: Basic calcium phosphate (BCP) and monosodium urate (MSU) crystals are particulates with potent pro-inflammatory effects, associated with osteoarthritis (OA) and gout, respectively. Bone erosion, due to increased osteoclastogenesis, is a hallmark of both arthropathies and results in severe joint destruction. The aim of this study was to investigate the effect of these endogenous particulates on anti-osteoclastogenic cytokine signalling.

Methods: Human osteoclast precursors (OcP) were treated with BCP and MSU crystals prior to stimulation with Interleukin (IL-6) or Interferon (IFN- γ) and the effect on Signal Transducer and Activator of Transcription (STAT)-3 and STAT-1 activation in addition to Mitogen Activated Protein Kinase (MAPK) activation was examined by immunoblotting. Crystal-induced suppressor of cytokine signalling (SOCS) protein and SH-2 containing tyrosine phosphatase (SHP) expression was assessed by real-time polymerase chain reaction (PCR) in the presence and absence of MAPK inhibitors.

Results: Pre-treatment with BCP or MSU crystals for 1 h inhibited IL-6-induced STAT-3 activation in human OcP, while pre-treatment for 3 h inhibited IFN- γ -induced STAT-1 activation. Both crystals activated p38 and extracellular signal-regulated (ERK) MAPKs with BCP crystals also activating c-Jun N-terminal kinase (JNK). Inhibition of p38 counteracted the inhibitory effect of BCP and MSU crystals and restored STAT-3 phosphorylation. In contrast, STAT-1 phosphorylation was not restored by MAPK inhibition. Finally, both crystals potently induced the expression of SOCS-3 in a MAPK dependent manner, while BCP crystals also induced expression of SHP-1 and SHP-2.

Conclusion: This study provides further insight into the pathogenic effects of endogenous particulates in joint arthropathies and demonstrates how they may contribute to bone erosion via the inhibition of anti-osteoclastogenic cytokine signalling. Potential targets to overcome these effects include p38 MAPK, SOCS-3 and SHP phosphatases.

© 2016 Osteoarthritis Research Society International. Published by Elsevier Ltd. All rights reserved.

Introduction

A number of studies have demonstrated that endogenous particulates such as gout-associated monosodium urate (MSU) crystals and osteoarthritis (OA)-associated basic calcium phosphate (BCP) crystals contribute to joint inflammation primarily through the production of pro-inflammatory cytokines and cartilage-degrading

enzymes. MSU crystals, arising as a result of persistent hyperuricaemia, induce matrix metalloproteinase (MMP) expression by chondrocytes¹ and Tumor Necrosis Factor (TNF)- α and IL-8 production by monocytes. However, the acute joint inflammation observed is primarily driven by macrophages, through the activation of a large multi-protein complex called the inflammasome which culminates in the activation of IL-1 β , a master regulator of local and systemic inflammation^{2–6}. Intra-articular BCP crystals activate and promote mitogenesis in osteoarthritic synovial fibroblasts and upregulate MMP expression by chondrocytes^{7,8}. In terms of cytokine production, they have been shown to induce IL-6 by chondrocytes⁹ as well as TNF- α and IL-1 β production by macrophages^{10–13}. Both BCP and MSU crystals induce the production of

* Address correspondence and reprint requests to: A. Dunne, School of Biochemistry & Immunology and School of Medicine, Trinity Biomedical Sciences Institute, Trinity College Dublin, Ireland. Fax: 353 1 6772400.

E-mail addresses: cunnincc@tcd.ie (C.C. Cunningham), emcorr@tcd.ie (E.M. Corr), g.mccarthy@ucd.ie (G.M. McCarthy), aidunne@tcd.ie (A. Dunne).

prostaglandin E2 (PGE2) by fibroblasts^{14,15}. Importantly, PGE2 was shown to promote osteoclastogenesis in a co-culture of murine osteoblasts and osteoclast precursors cells (OcP)¹⁶, while TNF α and IL-1 β were reported to upregulate the expression of RANKL by osteoblasts and synovial fibroblasts, thus promoting osteoclastogenesis through the activation of RANK-expressing OcP¹⁷. We have recently demonstrated that, in addition to the inflammasome, BCP crystals activate membrane-proximal kinases leading to the upregulation of damage-associated molecules, such as S100 proteins, which may contribute further to joint degradation¹³. Therefore, components of the inflammasome, as well as tyrosine kinases, represent potential therapeutic targets for the treatment of crystal-related arthropathies.

Despite recent advances in OA research, the complex processes involved in OA pathogenesis have hindered the development of a successful disease-modifying drug. As the disease progresses, increased cartilage permeability allows for signals to be transmitted from the synovial fluid and cartilage to the underlying subchondral bone. This may account for the observed bone deterioration and sclerosis or the formation of osteophytes and bone cysts, hallmarks of OA progression resulting from altered osteoclast activity^{18,19}. Bone erosion is also a common feature of tophaceous gout whereby granulomatous lesions, known as tophi, develop around a core of MSU crystals and tartrate-resistant acid phosphatase (TRAP) positive “osteoclast-like” cells have been identified within the tophus and at sites of bone erosion in gout patients^{20,21}.

Cytokines act directly on OcP and, depending on the stage of osteoclastogenesis, may promote or inhibit their differentiation. For example, TNF- α is pro-osteoclastogenic in the early stage of differentiation but anti-osteoclastogenic at the later stage, while IL-1 β is pro-osteoclastogenic at both stages²². IL-6 and IFN- γ are also associated with OA and gout, however, due to their pleiotropic nature, the precise role of these cytokines in osteoclastogenesis has been difficult to elucidate^{23–25}. IL-6 is reported to work synergistically with TNF- α to induce the formation of “osteoclast-like” cells from OcP both *in vitro* and *in vivo*²⁶. On the other hand, IL-6-deficient mice were shown to exhibit advanced osteoarthritic changes upon aging²⁷ while administration of recombinant IL-6 resulted in reduced cartilage destruction²⁸. Furthermore, IL-6 transgenic mice display decreased osteoclast numbers and decreased bone turnover, further supporting a role for IL-6 in the suppression of osteoclastogenesis²⁹. IFN- γ is suggested to act on T cells to induce the secretion of RANKL and TNF- α which promote osteoclastogenesis³⁰. Conversely, IFN- γ has been reported to inhibit RANKL signalling in OcP through the rapid degradation of TRAF6 and consequent inhibition of NF- κ B and JNK³¹. Additionally, it has been demonstrated that IFN- γ can inhibit IL-1-induced MMP-13 expression and this effect is diminished in OA chondrocytes compared to healthy chondrocytes due to reduced IFN- γ receptor expression³² thus providing further evidence that this cytokine may negatively regulate destructive processes in the joint.

In addition to endogenous particulates, it is well established that wear debris such as poly (methyl methacrylate) (PMMA) bone cement and titanium particles generated from orthopaedic implants can drive inflammation in the joint. This leads to increased osteoclastogenesis resulting in periprosthetic osteolysis and eventual implant failure^{33–36}. Furthermore, it has been demonstrated that, in addition to driving inflammation, both particulates can inhibit anti-osteoclastogenic signalling by IL-6 *via* the induction of suppressor of cytokine signalling (SOCS)-3, which negatively regulates IL-6-induced STAT-3 signalling. In the same study, titanium particles also inhibited IFN- γ -induced STAT-1 activation but failed to significantly induce the expression of SOCS-1, a key negative regulator of STAT-1 activity. Thus, the inhibition of STAT-1 signalling was believed to be SOCS-1-independent³⁷.

Further insight into the mechanisms by which endogenous particulates exert their effects will contribute to our understanding of the pathological processes associated with crystal deposition. In this study, we sought to determine if BCP and MSU crystals have the capacity to inhibit anti-osteoclastogenic cytokine signalling. We report that, similar to PMMA bone cement, both particulates are capable of inhibiting IL-6/IFN- γ -dependent STAT activation in human OcP. Furthermore, we demonstrate that this occurs primarily *via* the p38 mitogen-activated protein kinase (MAPK) and the upregulation of SOCS proteins. Finally, we demonstrate that BCP crystals upregulate the protein tyrosine phosphatases, SH2-containing tyrosine phosphatase (SHP)-1 and SHP-2 which may represent an additional mechanism by which particulates can inhibit anti-osteoclastogenic JAK/STAT signalling.

Materials and methods

Reagents

The Syk inhibitor (R788) was obtained from AdooQ BioScience (Irvine, CA), p38 (SB203580), JNK (SP600125), MEK/ERK (PD98059) inhibitors and MSU crystals were from Invivogen (San Diego, CA). PMMA particles (diameter range 1–10 μ m) were obtained from Polysciences, Inc. (Warrington, PA). BCP crystals in the form of hydroxyapatite (HA) were synthesized by alkaline hydrolysis of brushite as described³⁸. Recombinant human IL-6 and IFN- γ were obtained from Miltenyi Biotec (Bergisch Gladbach, Germany). Recombinant human M-CSF and RANKL were from PeproTech (Rocky Hill, NJ). Lymphoprep was obtained from Stemcell Technologies (Grenoble, France). All primary antibodies were obtained from Cell Signaling Technology (Beverly, Massachusetts). Secondary antibodies, cell culture reagents, Acid Phosphatase, Leukocyte (TRAP) Kit and all chemicals were from Sigma–Aldrich (St. Louis, Missouri).

Culture of OcP

Peripheral blood mononuclear cells (PBMC) were isolated by density gradient centrifugation from leukocyte-enriched buffy coats from anonymous healthy donors, obtained with permission from the Irish Blood Transfusion Board, St. James's Hospital, Dublin. CD14⁺ myeloid cells were positively selected from PBMC using anti-CD14 magnetic beads (Miltenyi Biotec, Bergisch Gladbach, Germany) and shown to be >90% pure, as determined by flow cytometry. CD14⁺ cells were cultured overnight in sterile petri dishes (10 \times 10⁶ cells/dish) in RPMI 1640 medium supplemented with 1% penicillin–streptomycin and 10% Foetal Bovine Serum and containing M-CSF (10 ng/ml). Cells were harvested and recultured overnight in RPMI containing M-CSF (10 ng/ml) in 6-well plates (for immunoblotting assays) or 24-well plates (for real-time polymerase chain reaction (PCR)). Consistent with previous reports^{37,39}, these cells are considered to be OcP due to their ability to differentiate into osteoclasts in the presence of RANKL. Late OcP were obtained by further differentiation with M-CSF (25 ng/ml) and RANKL (100 ng/ml) for 48 h. Mature, multinucleated (three or more nuclei), TRAP-positive osteoclasts were obtained after 14 days of culture, with replacement of RPMI (containing M-CSF and RANKL) every 3 days. Cells were counted under a microscope at three predetermined sites of area 0.3 \times 0.4 mm and a mean value (per donor) was calculated ($n = 3$ healthy donors).

Cell treatments

MAPK activation

OcP (1.5 \times 10⁶ cells/well) were stimulated with BCP crystals (100 μ g/ml), PMMA particles (500 μ g/ml) or MSU crystals (100 μ g/ml).

ml) for 15, 30 or 45 min (these concentrations were used throughout). Cells were lysed by addition of RIPA buffer (Tris 50 mM; NaCl 150 mM; SDS 0.1%; sodium deoxycholate 0.5 %; Triton X 100) containing phosphatase inhibitor cocktail 3 (Sigma–Aldrich). Lysates were electrophoresed on a 12% SDS-polyacrylamide gel and transferred to PVDF membranes (Millipore, Billerica, Massachusetts) prior to detection with anti-phospho-p38, anti-phospho-JNK or anti-phospho-ERK.

STAT activation

OcP (1.5×10^6 cells/well) were treated with PMMA particles, BCP or MSU crystals for the indicated times and stimulated with IL-6 (25 ng/ml) or IFN- γ (1.5 U/ml) for 12 min. To investigate the

role of Syk or MAPKs in STAT activation, cells were pre-treated for 45 min with inhibitors of Syk (R788, 2.5 μ M), p38 (SB203580, 10 μ M), JNK (SP600125, 20 μ M) or MEK/ERK (PD98059, 10 μ M) prior to treatment with BCP/MSU crystals for the indicated time points followed by IL-6/IFN- γ stimulation for 12 min. Cell lysates were prepared and electrophoresed, as previously described, prior to detection with anti-phospho-STAT-1 or anti-phospho-STAT-3.

SOCS/SHP induction

OcP were treated with BCP or MSU crystals for indicated time points. To investigate the role of Syk or MAPKs in SOCS induction, OcP were pre-treated with the aforementioned inhibitors prior to

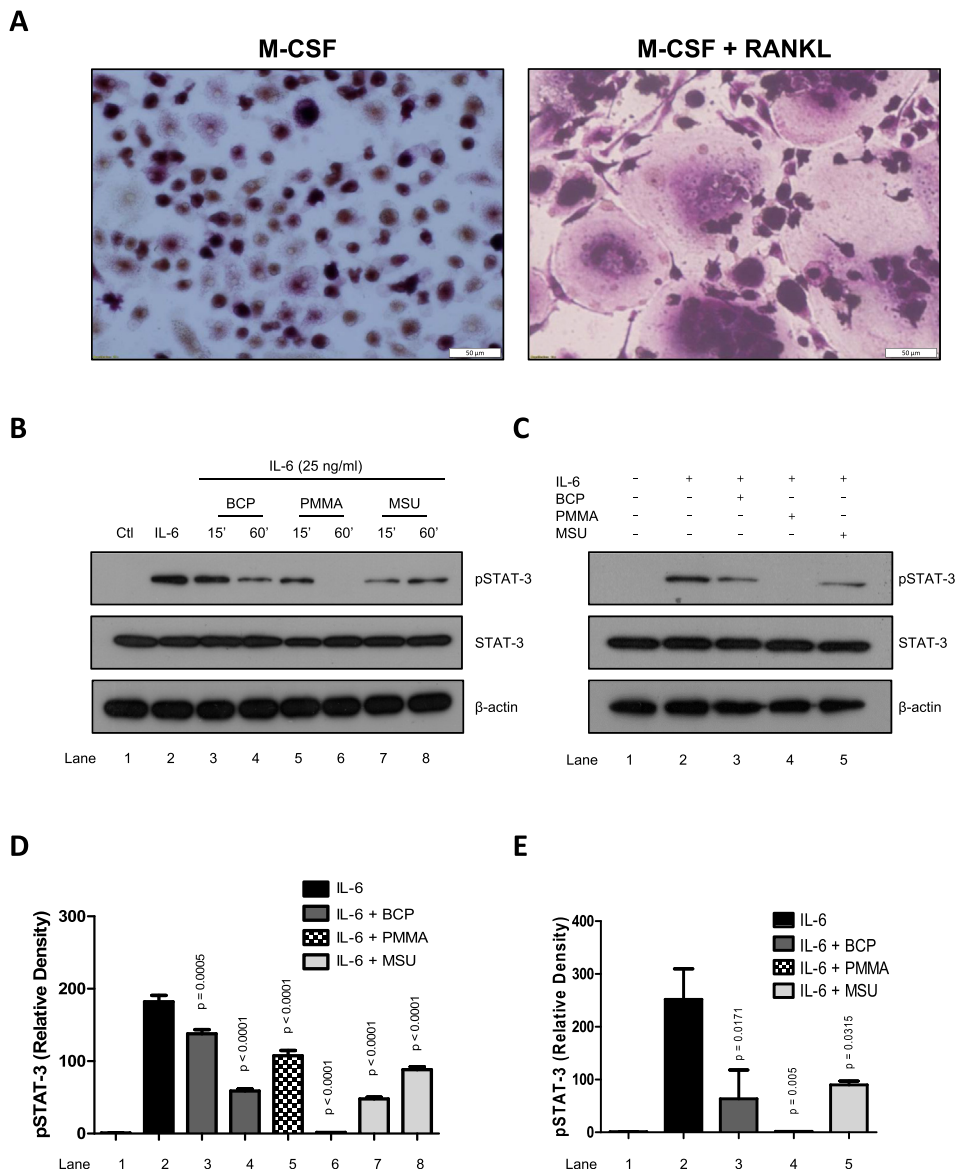


Fig. 1. BCP and MSU crystals inhibit IL-6-induced STAT-3 activation in early and late human OcP. (A) Human CD14⁺ cells (1.5×10^6 cells/well) were cultured with recombinant human M-CSF (25 ng/ml) alone or with M-CSF and RANKL (100 ng/ml) together for 14 days and stained for TRAP. (B) Human OcP were treated with BCP crystals (100 μ g/ml), PMMA particles (500 μ g/ml) or MSU crystals (100 μ g/ml) for 15 min (15') or 1 h (60') prior to stimulation with IL-6 (25 ng/ml) for 12 min. (C) Human OcP were cultured with M-CSF (25 ng/ml) and recombinant human RANKL (100 ng/ml) for 48 h and these 'late OcP' were treated with BCP crystals (100 μ g/ml), PMMA particles (500 μ g/ml) or MSU crystals (100 μ g/ml) for 1 h prior to stimulation with IL-6 (25 ng/ml) for 12 min. Phosphorylation of STAT-3 was detected by western blot using a phospho-specific antibody. Representative western blots of three independent experiments are shown ($n = 3$ healthy donors). (D, E) Densitometric analysis of three western blots was performed using ImageJ software. Bar graphs illustrate the mean (\pm S.E.M.) increase in phosphorylation following each treatment, relative to the untreated sample (Ctl) and normalised to total STAT-3 protein. Statistical analysis of each condition vs IL-6 alone (Lane 2) was performed using a one way ANOVA with Tukey post-test.

stimulation with BCP/MSU crystals for 3 h. Gene expression was analysed by real-time PCR.

Real-time PCR

RNA was extracted from OcP using High Pure RNA Isolation Kits (Roche, Basel, Switzerland) and assessed for concentration and purity using the NanoDrop 2000c UV–Vis spectrophotometer. RNA was equalised and reverse transcribed using the Applied Biosystems High-Capacity cDNA Reverse Transcription Kit. Real-time PCR was carried out on triplicate cDNA samples using the CFX96 Touch Real-Time PCR Detection System (Bio-Rad Laboratories, Hercules, California). Reactions included iTaq Universal SYBR Green Supermix (Bio-Rad Laboratories), cDNA and forward and reverse primers (250 nM). mRNA amounts were normalised relative to the housekeeping gene, Ribosomal Protein S15 (RPS15). Oligonucleotide primer sequences:

RPS15 sense: 5'-CGGACCAAAGCGATCTCTTC-3'
 RPS15 anti-sense: 5'-CGCACTGTACAGCTGCATCA-3'
 SOCS-1 sense: 5'-CACTTCCGCACATTCGGTTC-3'
 SOCS-1 anti-sense: 5'-AGGGGAAGGAGCTCAGGTA-3'
 SOCS-3 sense: 5'-ATCCTGGTGACATGCTCCTC-3'
 SOCS-3 anti-sense: 5'-CAAATGTTGCTTCCCCTTA-3'

Statistical analysis

All experiments were run at least three times (three technical replicates were used for real-time PCR and $n \geq 3$ healthy donors). Dot plots represent mean \pm 95% confidence intervals (CI). Statistical analysis was performed by one way analysis of variance (ANOVA) with Tukey post-test (where applicable) or two-tailed unpaired *t*-test on GraphPad Prism 6 software. *P* value ≤ 0.05 was deemed statistically significant.

Results

BCP and MSU crystals inhibit IL-6 signalling in human OcP

Human OcP were prepared as described previously³⁹. Their ability to differentiate into mature osteoclasts was confirmed upon treatment of these cells with M-CSF and RANKL for 14 days. OcP cultured in M-CSF alone displayed weak TRAP staining and did not form giant multinucleated cells while those cultured in the presence of M-CSF and RANKL together formed giant TRAP⁺ multinucleated cells [Fig. 1(A)]. IL-6 exerts anti-osteoclastogenic effects on human OcP via activation of STAT-3 and both PMMA and titanium particles have been reported to inhibit this activity³⁷. In order to examine the effect of endogenous particles on IL-6 signalling, human OcP were treated with BCP crystals, PMMA particles or MSU crystals for 15 min or 1 h prior to stimulation with IL-6 (25 ng/ml) for 12 min. Activation of STAT-3, as indicated by phosphorylation, was examined by western blot [Fig. 1(B)]. IL-6 induced a robust increase in phosphorylation of STAT-3 (Lane 2) which was slightly reduced by pre-treatment with BCP crystals for 15 min (Lane 3) and even more so by pre-treatment for 1 h (Lane 4). Consistent with previous reports, PMMA particle pre-treatment for 15 min reduced STAT-3 activation (Lane 5) while pre-treatment for 1 h completely abolished STAT-3 phosphorylation (Lane 6). Additionally, MSU crystal pre-treatment for 15 min (Lane 7) or 1 h (Lane 8) greatly reduced STAT-3 activation. This effect was also observed in late OcP in which osteoclast differentiation had been initiated by prior addition of RANKL [Fig. 1(C)]. As observed previously, both BCP and MSU crystals reduced STAT-3 phosphorylation following IL-6 stimulation, while PMMA particles completely

inhibited STAT-3 phosphorylation. Densitometric analysis of three western blots is shown for both early [Fig. 1(D)] and late [Fig. 1(E)] OcP. This demonstrates that, like wear debris particles, endogenous particulates such as BCP and MSU crystals can inhibit IL-6 signalling in OcP.

BCP and MSU crystals inhibit IFN- γ signalling in human OcP

IFN- γ is believed to exert anti-osteoclastogenic effects on OcP through activation of the IFN- γ receptor which initiates JAK/STAT signalling resulting in STAT-1 phosphorylation³¹. Titanium particles have previously been reported to inhibit STAT-1 activation³⁷ and, having observed that BCP and MSU crystals interfere with IL-6 signalling, the effect of these endogenous crystals on IFN- γ signalling was next investigated. Human OcP were treated with both forms of crystals as well as PMMA particles for 1 or 3 h prior to stimulation with IFN- γ for 12 min. Activation of STAT-1, as indicated by phosphorylation, was examined by western blot [Fig. 2(A)]. Consistent with previous reports, IFN- γ induced the phosphorylation of STAT-1 (Lane 2). While pre-treatment with BCP crystals (Lane 3), PMMA particles (Lane 5) or MSU crystals (Lane 7) for 1 h did not appear to affect STAT-1 activation, pre-treatment for 3 h (Lanes 4, 6 and 8) greatly inhibited IFN- γ -induced STAT-1 phosphorylation. Densitometric analysis of three western blots revealed that MSU crystals exerted the greatest inhibitory effect following 3 h of stimulation, followed by PMMA particles and finally, BCP crystals [Fig. 2(B)]. This suggests that, as with IL-6, both wear debris and endogenous particles can inhibit anti-osteoclastogenic IFN- γ signalling in OcP.

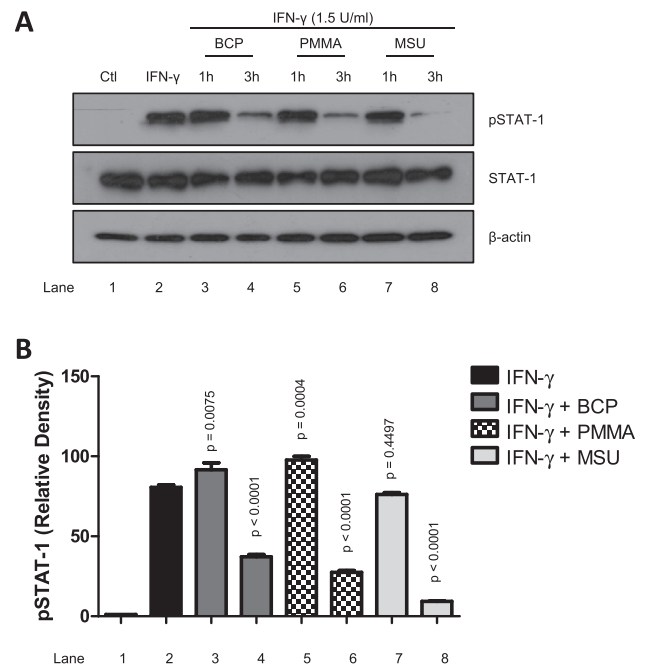


Fig. 2. BCP and MSU crystals inhibit IFN- γ -induced STAT-1 activation in human OcP. (A) Human OcP (1.5×10^6 cells/well) were treated with BCP crystals (100 μ g/ml), PMMA particles (500 μ g/ml) or MSU crystals (100 μ g/ml) for 1 h (1 h) or 3 h (3 h) prior to stimulation with IFN- γ (1.5 U/ml) for 12 min. Phosphorylation of STAT-1 was detected by western blot using a phospho-specific antibody. A representative western blot of three independent experiments is shown ($n = 3$ healthy donors). (B) Densitometric analysis of three western blots was performed using ImageJ software. Bar graph illustrates the mean increase (\pm S.E.M.) in phosphorylation following each treatment, relative to the untreated sample (Ctl) and normalised to total STAT-1 protein. Statistical analysis of each condition vs IFN- γ alone (Lane 2) was performed using a one way ANOVA with Tukey post-test.

BCP and MSU crystals activate MAPKs in human OcP

Activation of the p38, ERK and JNK MAPK pathways is required to induce the nuclear translocation of transcription factors in order to initiate the transcription of osteoclast-specific genes^{40,41}. We have previously reported that BCP crystals activate ERK in human synovial fibroblasts¹³, while PMMA and titanium particles have been reported to activate all three MAPKs in human OcP³⁷. The

effect of endogenous particles on MAPK activation in human OcP, however, has not yet been reported. In order to investigate this, human OcP were stimulated with BCP crystals, PMMA particles and MSU crystals for 15, 30 and 45 min. Activation of MAPKs, as indicated by phosphorylation was examined by western blot. All three particle types induced the phosphorylation of p38 at each time point tested, with BCP crystals having the most potent effect. MSU-induced ERK phosphorylation was only evident after 15 min while

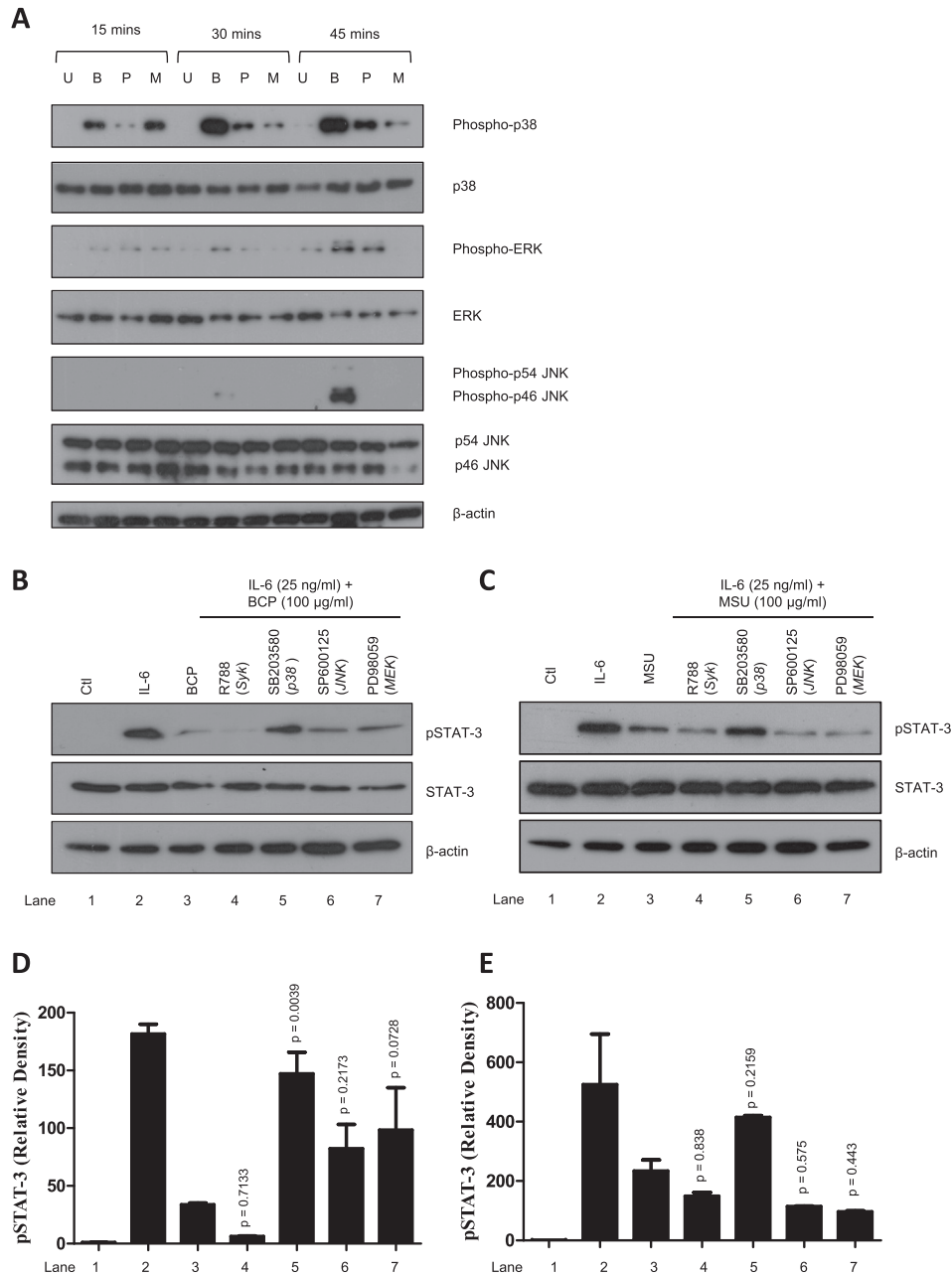


Fig. 3. BCP and MSU crystals activate MAPKs and inhibit STAT-3 phosphorylation in human OcP in a MAPK-dependent manner. (A) Human OcP (1.5×10^6 cells/well) were untreated (U) or stimulated with BCP (B) crystals (100 μg/ml), PMMA (P) particles (500 μg/ml) or MSU (M) crystals (100 μg/ml) for 15, 30 or 45 min. Phosphorylation of p38, ERK and JNK was detected by western blot using phospho-specific antibodies. A representative western blot of three independent experiments is shown ($n = 3$ healthy donors). Human OcP (1.5×10^6 cells/well) were pre-treated with inhibitors of Syk (R788, 2.5 μM), p38 (SB203580, 10 μM), JNK (SP600125, 20 μM) or MEK (PD98059, 10 μM) for 45 min prior to treatment with (B, D) BCP crystals (100 μg/ml) or (C, E) MSU crystals (100 μg/ml) for 1 h and stimulation with IL-6 (25 ng/ml) for 12 min. Phosphorylation of STAT-3 was detected by western blot using a phospho-specific antibody. Representative western blots of three independent experiments are shown ($n = 3$ healthy donors). Densitometric analysis of three western blots was performed using ImageJ software. (D, E) Bar graphs illustrate the mean (\pm S.E.M.) increase in phosphorylation following each treatment, relative to the untreated sample (Ctl) and normalised to total STAT-3 protein. Statistical analysis of each condition vs IL-6 + BCP/MSU (Lane 3) was performed using a one way ANOVA with Tukey post-test.

BCP crystal- and PMMA particle-induced phosphorylation was maximal at 45 min. Activation of JNK was observed only in the BCP-treated samples with maximal phosphorylation at 45 min post-stimulation [Fig. 3(A)].

Having observed that BCP and MSU crystals potentially activate MAPKs, particularly p38, in human OcP, the involvement of MAPKs in BCP/MSU crystal-mediated inhibition of IL-6 signalling was next investigated. Human OcP were pre-treated with inhibitors of p38 (SB203580), MEK (PD98059) and JNK (SP600125) MAPKs for 45 min prior to treatment with BCP or MSU crystals for 1 h and stimulation with IL-6 for 12 min. The Syk inhibitor (R788) was also included as we have previously demonstrated that BCP crystals activate this kinase¹³. Activation of STAT-3, as indicated by phosphorylation, was examined by western blot [Fig. 3(B)]. Consistent with previous observations, IL-6 induced the phosphorylation of STAT-3 (Lane 2), which was inhibited by pre-treatment with BCP crystals (Lane 3). Treatment with the Syk inhibitor prior to BCP stimulation did not prevent the inhibition of STAT-3 phosphorylation by BCP crystals (Lane 4), while treatment with the p38 inhibitor greatly reduced the ability of BCP crystals to inhibit STAT-3 phosphorylation (Lane 5) and inhibition of JNK (Lane 6) and ERK (Lane 7) slightly restored STAT-3 phosphorylation. Similarly, MSU-mediated inhibition of IL-6-induced STAT-3 phosphorylation was prevented by pre-treatment with the p38 inhibitor while the ERK and JNK MAPK inhibitors had no effect [Fig. 3(C)]. Densitometric analysis of three western blots revealed that p38 inhibition had the greatest effect [Fig. 3(D) and (E)], suggesting that p38 plays a predominant role in BCP and MSU crystal-mediated inhibition of IL-6 signalling.

BCP and MSU crystals upregulate SOCS-3 expression in human OcP

A well-known mechanism for the downregulation of JAK/STAT signalling is *via* the induction of the SOCS family of cytokine suppressors. SOCS-3 is transcribed by STAT-3 and regulates STAT-3 activation through the formation of a negative feedback loop⁴². Both PMMA and titanium particles have previously been reported to induce SOCS-3 expression which potentially downregulates IL-6 signalling through the inhibition of STAT-3 activity³⁷. To determine whether BCP and MSU crystals inhibit STAT-3 *via* the upregulation of SOCS-3, human OcP were stimulated with BCP or MSU crystals for 1 or 3 h and expression of SOCS-3 was analysed by real-time PCR. Both crystal types induced SOCS-3 at 1 h while a greater induction was observed at 3 h post-stimulation (data not shown). This time point was employed to investigate whether BCP/MSU crystal-induced SOCS-3 upregulation is MAPK-dependent. Human OcP were treated with inhibitors of p38 (SB203580), MEK (PD98059) and JNK (SP600125) MAPKs or Syk (R788) for 45 min prior to crystal treatment and expression of SOCS-3 was analysed by real-time PCR [Fig. 4(A)]. Again, BCP crystals significantly induced ($P = 0.0016$) SOCS-3 at the mRNA level. Pre-treatment with either the Syk or ERK inhibitor had no discernible effect on BCP crystal-induced SOCS-3 expression [Fig. 4(A)] and, while a slight reduction was observed, inhibition of JNK had no significant effect ($P = 0.3913$). However, pre-treatment with the p38 inhibitor significantly ($P = 0.0088$) prevented the upregulation of SOCS-3 by BCP crystals. This result suggests that BCP crystals upregulate SOCS-3 primarily through the activation of p38 and reflects the previous observation whereby p38-inhibition restored STAT-3 phosphorylation. Similarly, inhibition of p38 significantly ($P = 0.0043$) prevented the induction of SOCS-3 by MSU crystals and inhibition of ERK also markedly reduced SOCS-3 expression [Fig. 4(B)]. This suggests that both ERK and p38 may play a role in MSU-induced SOCS-3 expression, however, p38 appears to be the predominant MAPK involved.

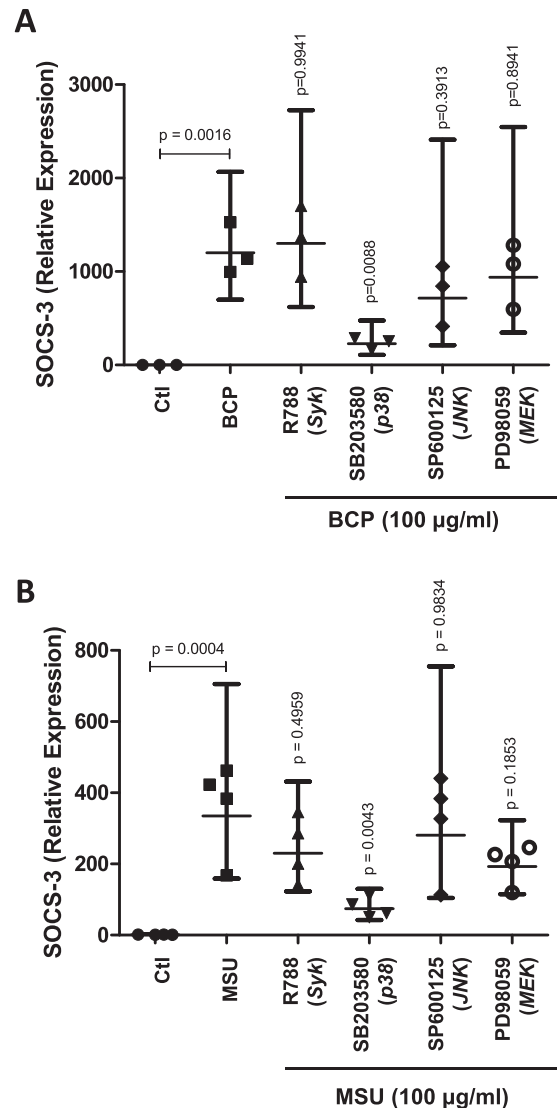


Fig. 4. BCP and MSU crystals induce SOCS-3 expression in human OcP in a MAPK-dependent manner. Human OcP (0.25×10^6 cells/well) were pre-treated with inhibitors of Syk (R788, 2.5 µM), p38 (SB203580, 10 µM), JNK (SP600125, 20 µM) or MEK (PD98059, 10 µM) for 45 min prior to treatment with (A) BCP crystals (100 µg/ml) or (B) MSU crystals (100 µg/ml) for 3 h. RNA was extracted and mRNA levels of SOCS-3 were analysed by real-time PCR. Results shown are mean \pm 95% CI of three to four independent experiments ($n = 3-4$ healthy donors; three/four cultures with three technical replicates). Statistical analysis of each condition vs BCP/MSU alone was performed using a one way ANOVA with Tukey post-test.

BCP and MSU crystals inhibit STAT-1 phosphorylation in human OcP in a MAPK-independent manner

Similar to STAT-3, STAT-1 is also regulated by SOCS proteins. Specifically, SOCS-1 is induced by STAT-1 to form a negative feedback loop which regulates IFN- γ signalling by STAT-1^{42,43}. To determine whether crystal-mediated inhibition of STAT-1 phosphorylation occurs as a result of SOCS-1 induction, human OcP were stimulated with BCP or MSU crystals and expression of SOCS-1 was analysed by real-time PCR. Stimulation with the crystals for 1 h did not induce a significant increase in SOCS-1 expression (data not shown) and, while expression was increased to a greater extent at 3 h post-stimulation with BCP ($P = 0.0033$) and MSU ($P = 0.0811$) crystals [Fig. 5(A)], the effects were less pronounced when compared to SOCS-3 induction. Furthermore, neither BCP- nor MSU-mediated

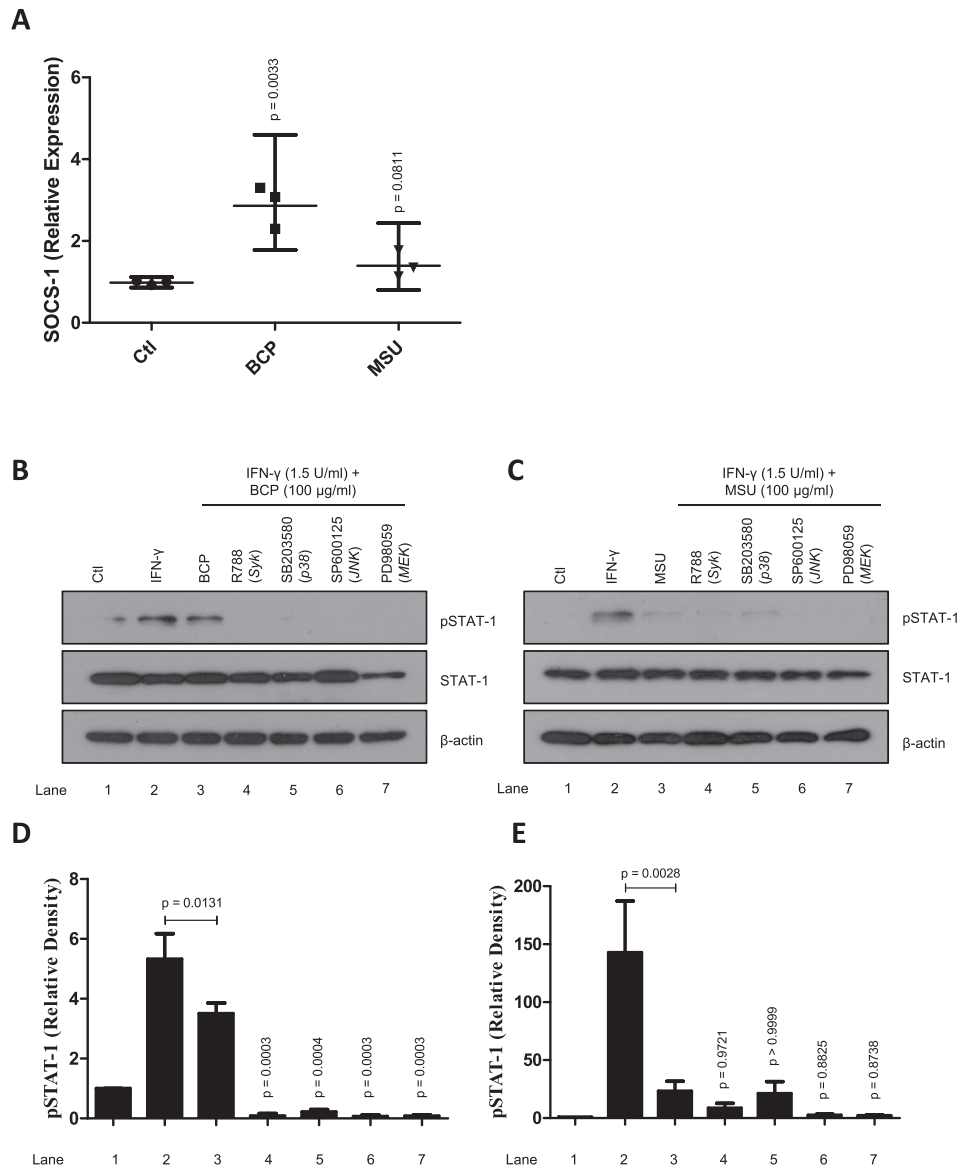


Fig. 5. BCP and MSU crystals inhibit STAT-1 phosphorylation in human Ocp in a MAPK-independent manner. (A) Human Ocp (0.25×10^6 cells/well) were treated with BCP crystals (100 μ g/ml) or MSU crystals (100 μ g/ml) for 3 h, RNA was extracted and mRNA levels of SOCS-1 were analysed by real-time PCR. Results shown are mean \pm 95% CI of three independent experiments ($n = 3$ healthy donors; three cultures with three technical replicates). Statistical analysis of each condition vs untreated (Ctl) was performed using a two-tailed unpaired t test. Human Ocp (1.5×10^6 cells/well) were pre-treated with inhibitors of Syk (R788, 2.5 μ M), p38 (SB203580, 10 μ M), JNK (SP600125, 20 μ M) or MEK (PD98059, 10 μ M) for 45 min prior to treatment with (B, D) BCP crystals (100 μ g/ml) or (C, E) MSU crystals for 3 h and stimulation with IFN- γ (1.5 U/ml) for 12 min. Phosphorylation of STAT-1 was detected by western blot using a phospho-specific antibody. Representative western blots of three independent experiments are shown ($n = 3$ healthy donors). Densitometric analysis of three western blots was performed using ImageJ software. (D, E) Bar graphs illustrate the mean (\pm s.e.m.) increase in phosphorylation following each treatment, relative to the untreated sample (Ctl) and normalised to total STAT-1 protein. Statistical analysis of each condition vs IFN- γ + BCP/MSU (Lane 3) was performed using a one way ANOVA with Tukey post-test.

inhibition of IFN- γ -driven STAT-1 phosphorylation was overcome by MAPK inhibition [Fig. 5(B)–(E)]. These results suggest that STAT-1 inhibition is MAPK-independent and while BCP and MSU crystals can induce SOCS-1 expression, this may not be the primary mechanism by which the particles inhibit IFN- γ signalling.

BCP crystals upregulate SHP-1 and SHP-2 in human Ocp

Another potential mechanism for the inhibition of STAT-1 activation is via the induction of tyrosine phosphatases, such as SHP-1 and SHP-2, which dephosphorylate the cytoplasmic chain of the IFN- γ receptor, as well as associated JAKs, thus preventing the JAK-dependent phosphorylation of STAT-1⁴⁴. To examine whether endogenous particulates can modulate SHP expression, human Ocp

were stimulated with BCP or MSU crystals for 1, 3 and 24 h and gene expression was analysed by real-time PCR. MSU crystals had no significant effect on SHP expression (data not shown), however, BCP crystals significantly increased SHP-1 expression at the 1 ($P = 0.0246$) and 3 h ($P = 0.0426$) time points [Fig. 6(A)] while SHP-2 induction ranged between 15 and 150 fold over untreated cells [Fig. 6(B)].

BCP and MSU crystals counteract the anti-osteoclastogenic effects of IL-6 and IFN- γ

To determine whether crystal-mediated inhibition of IL-6 and IFN- γ signalling prevents the anti-osteoclastogenic effects of these cytokines, Ocp were cultured for 14 days in the presence of

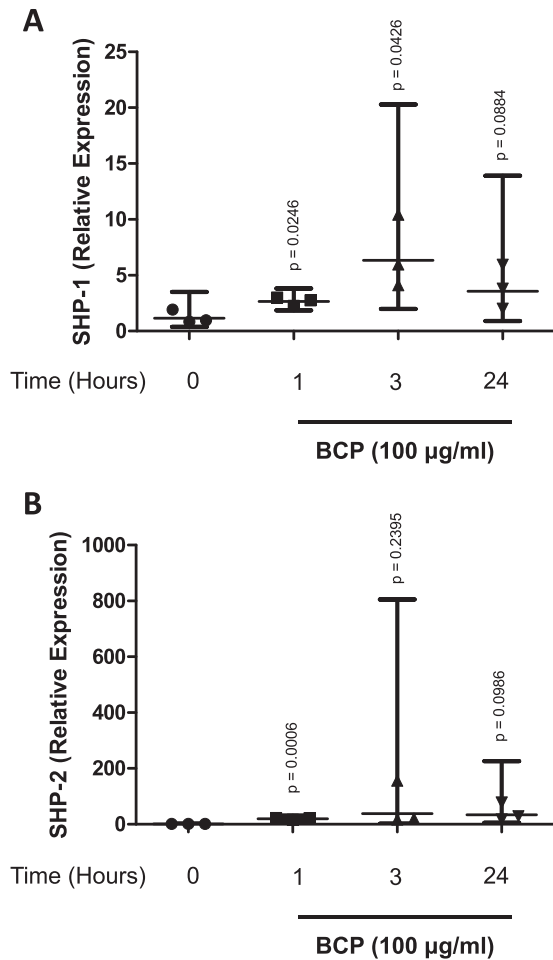


Fig. 6. BCP crystals upregulate SHP-1 and SHP-2 in human OcP. Human OcP (0.25×10^6 cells/well) were treated with BCP crystals (100 $\mu\text{g/ml}$) for 1, 3 or 24 h. RNA was extracted and mRNA levels of (A) SHP-1 and (B) SHP-2 were analysed by real-time PCR. Results shown are mean \pm 95% CI of three independent experiments ($n = 3$ healthy donors; three cultures with three technical replicates). Statistical analysis of each condition vs untreated (Time 0 h) was performed using a one way ANOVA with Tukey post-test.

M-CSF and RANKL and treated with either IL-6 or IFN- γ in the presence or absence of BCP or MSU crystals. Treatment with IL-6 or IFN- γ reduced the formation of osteoclasts, as indicated by weaker TRAP staining and fewer giant multinucleated cells [Fig. 7(A)–(C)]. Interestingly, treatment with MSU or BCP crystals increased the number of giant, TRAP⁺ multinucleated cells thus counteracting the inhibition of osteoclastogenesis by IL-6 [Fig. 7(A), lower panel] and IFN- γ [Fig. 7(B), lower panel]. This supports the hypothesis that endogenous particulates contribute to destructive processes in the joint, not only *via* their action on chondrocytes, fibroblasts and macrophages but also through their action on OcP.

Discussion

The progressive joint destruction associated with OA and tophaceous gout is driven by chronic inflammation and excessive osteoclastogenesis^{19,45}. Under physiological conditions, a balance between bone formation and resorption maintains skeletal homeostasis; however, in certain pathological states this balance is tipped in favour of osteoclast-mediated bone

resorption. The precise roles of the pleiotropic cytokines, IL-6 and IFN- γ , in osteoclastogenesis have been difficult to elucidate, as, depending on the cytokine milieu and target cells, both pro- and anti-osteoclastogenic effects have been reported. Direct interaction of IL-6 or IFN- γ with OcP appears to be largely anti-osteoclastogenic^{22,29,31,46,47}. In this study, we report that, similar to PMMA and titanium wear debris, both BCP and MSU crystals potentially inhibit JAK/STAT signalling by IL-6 potentially *via* the induction of SOCS-3, a well-established inhibitor of the JAK/STAT pathway, which is also induced by RANKL to mediate RANKL-dependent osteoclastogenesis^{37,48}. Upregulation of SOCS-3 by both BCP and MSU crystals was dependent on p38 MAPK and pharmacological inhibition of p38 could overcome the observed inhibition of IL-6-induced STAT-3 phosphorylation. In addition to p38, both BCP and MSU crystals activated ERK in human OcP, albeit to a lesser extent, while BCP crystals also induced the activation of JNK. Both crystal types also inhibited IFN- γ -induced STAT-1 phosphorylation, however, the effects on STAT-1 activation were MAPK-independent. Furthermore, while both particulates could induce the upregulation of SOCS-1, which is known to inhibit STAT-1 activation, the observed induction was far weaker than that seen for SOCS-3. This is in agreement with a previous study demonstrating that titanium particle-mediated inhibition of IFN- γ signalling is independent of MAPK activation and SOCS-1 induction³⁷. An alternative mechanism through which JAK/STAT signalling is inhibited is *via* protein phosphatases such as SHP-1 and SHP-2. We demonstrate for the first time that, in addition to SOCS proteins, BCP crystals can also upregulate the expression of SHP proteins in human OcP and that treatment of OcP with either MSU or BCP crystals could overcome the anti-osteoclastogenic effects of IL-6 and IFN- γ as evidenced by increased formation of TRAP⁺ multinucleated cells. A proposed model summarizing these findings is presented in Fig. 8. It has recently been reported that SHP-2 deficiency is associated with reduced fusion of OcP and decreased expression of osteoclastogenic markers, such as Cathepsin K and TRAP⁴⁹, therefore in addition to inhibiting anti-osteoclastogenic STAT-1 signalling, the upregulation of SHP proteins by BCP crystals may, in fact, promote osteoclastogenesis. Further study using specific SHP phosphatase inhibitors or SHP-deficient cells will validate the role of these proteins in particulate-induced responses. It should be noted that BCP crystals are composed mainly of hydroxyapatite which is commonly used as a biomimetic to coat orthopaedic implants⁵⁰. Hence, it is likely that, similar to PMMA and titanium particles, hydroxyapatite also contributes to implant loosening through periprosthetic inflammation and osteoclastogenesis.

With the ever-increasing burden of OA in an aging society, it is crucial that a better knowledge of host factors is obtained in order to develop a treatment which halts the destructive events that occur early on in OA and thus, prevents the disease from progressing. Similarly, the incidence of gout is increasing and, unlike BCP crystals, MSU crystals are easily detected in affected joints allowing for early diagnosis. Three important processes occur in degenerative arthropathies such as OA: the inflammatory response, the production of proteolytic enzymes and bone remodelling. By gaining a better understanding of the interplay between these processes, it may be possible to identify a key step in disease progression. While a range of cell types contribute to these processes, this study specifically focussed on the cells responsible for bone degeneration, with particular attention to the intracellular signalling pathways activated, or inhibited, by endogenous crystals. Though the effects of the crystals may be transient, elucidation of these pathways may lead to the identification of a crucial molecule which may then be targeted

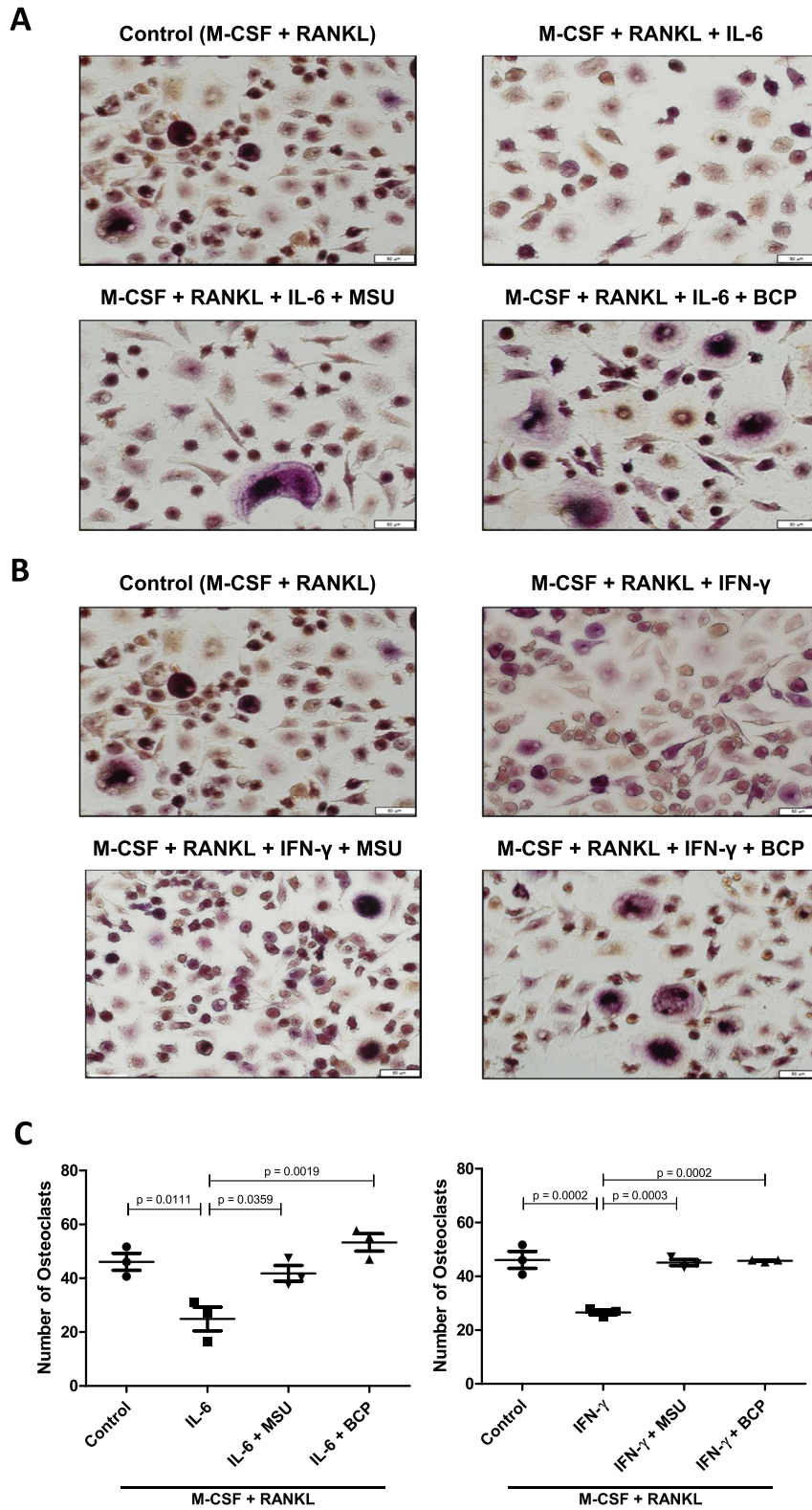


Fig. 7. BCP and MSU crystals counteract the anti-osteoclastogenic effects of IL-6 and IFN-γ. (A) Human CD14⁺ cells (0.5×10^6 cells/well) were cultured with recombinant human M-CSF (25 ng/ml) and RANKL (100 ng/ml) and treated every 3 days with IL-6 (25 ng/ml) alone, IL-6 and MSU crystals (100 μg/ml) or IL-6 and BCP crystals (100 μg/ml). (B) Human CD14⁺ cells (0.5×10^6 cells/well) were cultured with recombinant human M-CSF (25 ng/ml) and RANKL (100 ng/ml) and treated every 3 days with IFN-γ (1.5 U/ml) alone, IFN-γ and MSU crystals (100 μg/ml) or IFN-γ and BCP crystals (100 μg/ml). Cells were stained for TRAP after 14 days of culture. Representative images of three independent experiments are shown ($n = 3$ healthy donors). (C) Cells were counted under a microscope at three predetermined sites of area 0.3×0.4 mm and a mean value (per donor) was calculated. Results shown are mean \pm S.E.M. of three independent experiments ($n = 3$ healthy donors). Statistical analysis of each condition vs IL-6/IFN-γ alone was performed using a one way ANOVA with Tukey post-test.

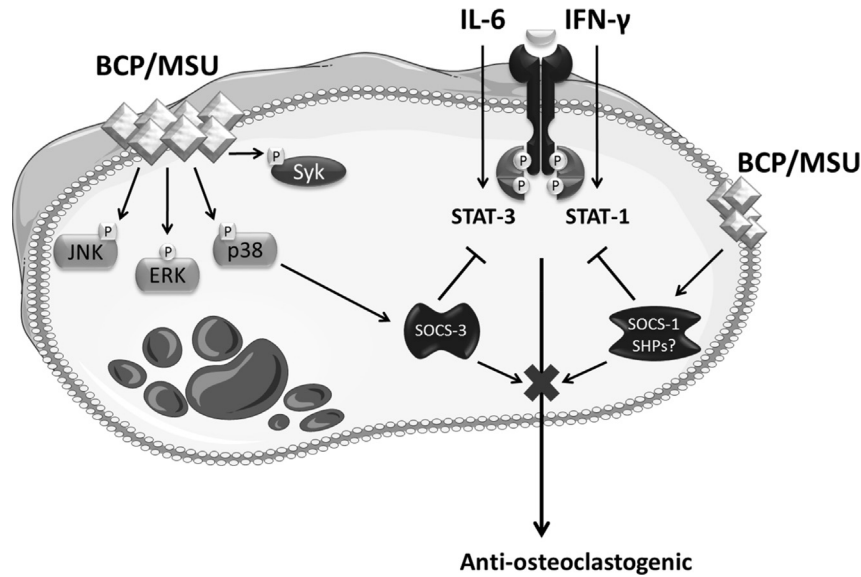


Fig. 8. Model illustrating proposed pathways activated or inhibited by endogenous particulates. Anti-osteoclastogenic signalling driven by IL-6 and/or IFN- γ is inhibited by MSU and BCP crystals via the upregulation of SOCS proteins which are known inhibitors of the JAK/STAT pathway. SOCS-3 induction occurs via crystal-induced p38 activation whereas MAP kinases do not appear to be involved in crystal-induced SOCS-1 expression. An alternative mode of inhibition may be mediated by members of the SHP tyrosine phosphatase family.

pharmacologically. Targeting synovial activation induced by crystal deposition may help to prevent the initiation of additional destructive processes, while targeting the osteoclastogenic effects of crystals may be beneficial in the prevention of increased bone remodelling.

Author contributions

CC and AD contributed to conception and design of the study, analysis and interpretation of the data, drafting of the article. EC contributed to the analysis and interpretation of the data, drafting of the article. GM contributed to the analysis and interpretation of the data, drafting of the article and provision of study materials.

Conflict of interest

The authors declare no conflicts of interest.

Funding

The study is supported by the Health Research Board, Ireland (Grant No.: HRA/POR/2012/20) and Trinity College Dublin.

References

- Liu R, Liote F, Rose DM, Merz D, Terkeltaub R. Proline-rich tyrosine kinase 2 and Src kinase signaling transduce monosodium urate crystal-induced nitric oxide production and matrix metalloproteinase 3 expression in chondrocytes. *Arthritis Rheum* 2004;50:247–58.
- Roddy E, Doherty M. Epidemiology of gout. *Arthritis Res Ther* 2010;12:223.
- Martinon F, Petrilli V, Mayor A, Tardivel A, Tschopp J. Gout-associated uric acid crystals activate the NALP3 inflammasome. *Nature* 2006;440:237–41.
- Terkeltaub R, Zachariae C, Santoro D, Martin J, Peveri P, Matsushima K. Monocyte-derived neutrophil chemotactic factor/interleukin-8 is a potential mediator of crystal-induced inflammation. *Arthritis Rheum* 1991;34:894–903.
- Liu-Bryan R, Liote F. Monosodium urate and calcium pyrophosphate dihydrate (CPPD) crystals, inflammation, and cellular signaling. *Joint Bone Spine* 2005;72:295–302.
- Kozin F, Ginsberg MH, Skosey JL. Polymorphonuclear leukocyte responses to monosodium urate crystals: modification by adsorbed serum proteins. *J Rheumatol* 1979;6:519–26.
- McCarthy GM, Westfall PR, Masuda I, Christopherson PA, Cheung HS, Mitchell PG. Basic calcium phosphate crystals activate human osteoarthritic synovial fibroblasts and induce matrix metalloproteinase-13 (collagenase-3) in adult porcine articular chondrocytes. *Ann Rheum Dis* 2001;60:399–406.
- Bai G, Howell DS, Howard GA, Roos BA, Cheung HS. Basic calcium phosphate crystals up-regulate metalloproteinases but down-regulate tissue inhibitor of metalloproteinase-1 and -2 in human fibroblasts. *Osteoarthritis Cartilage* 2001;9:416–22.
- Nasi S, So A, Combes C, Daudon M, Busso N. Interleukin-6 and chondrocyte mineralisation act in tandem to promote experimental osteoarthritis. *Ann Rheum Dis* 2016;75:1372–9.
- Nadra I, Mason JC, Philippidis P, Florey O, Smythe CD, McCarthy GM, et al. Proinflammatory activation of macrophages by basic calcium phosphate crystals via protein kinase C and MAP kinase pathways: a vicious cycle of inflammation and arterial calcification? *Circ Res* 2005;96:1248–56.
- Jin C, Frayssinet P, Pelker R, Cwirka D, Hu B, Vignery A, et al. NLRP3 inflammasome plays a critical role in the pathogenesis of hydroxyapatite-associated arthropathy. *Proc Natl Acad Sci USA* 2011;108:14867–72.
- Pazar B, Ea HK, Narayan S, Kolly L, Bagnoud N, Chobaz V, et al. Basic calcium phosphate crystals induce monocyte/macrophage IL-1 β secretion through the NLRP3 inflammasome *in vitro*. *J Immunol* 2011;186:2495–502.
- Cunningham CC, Mills E, Mielke LA, O'Farrell LK, Lavelle E, Mori A, et al. Osteoarthritis-associated basic calcium phosphate crystals induce pro-inflammatory cytokines and damage-associated molecules via activation of Syk and PI3 kinase. *Clin Immunol* 2012;144:228–36.
- Morgan MP, Whelan LC, Sallis JD, McCarthy CJ, Fitzgerald DJ, McCarthy GM. Basic calcium phosphate crystal-induced

- prostaglandin E2 production in human fibroblasts: role of cyclooxygenase 1, cyclooxygenase 2, and interleukin-1beta. *Arthritis Rheum* 2004;50:1642–9.
15. Wigley FM, Fine IT, Newcombe DS. The role of the human synovial fibroblast in monosodium urate crystal-induced synovitis. *J Rheumatol* 1983;10:602–11.
 16. Kaji H, Sugimoto T, Kanatani M, Fukase M, Kumegawa M, Chihara K. Prostaglandin E2 stimulates osteoclast-like cell formation and bone-resorbing activity via osteoblasts: role of cAMP-dependent protein kinase. *J Bone Miner Res* 1996;11:62–71.
 17. Wei S, Kitaura H, Zhou P, Ross FP, Teitelbaum SL. IL-1 mediates TNF-induced osteoclastogenesis. *J Clin Invest* 2005;115:282–90.
 18. Goldring MB, Goldring SR. Osteoarthritis. *J Cell Physiol* 2007;213:626–34.
 19. Li G, Yin J, Gao J, Cheng TS, Pavlos NJ, Zhang C, et al. Subchondral bone in osteoarthritis: insight into risk factors and microstructural changes. *Arthritis Res Ther* 2013;15:223.
 20. Dalbeth N, Pool B, Gamble GD, Smith T, Callon KE, McQueen FM, et al. Cellular characterization of the gouty tophus: a quantitative analysis. *Arthritis Rheum* 2010;62:1549–56.
 21. Dalbeth N, Clark B, Gregory K, Gamble G, Sheehan T, Doyle A, et al. Mechanisms of bone erosion in gout: a quantitative analysis using plain radiography and computed tomography. *Ann Rheum Dis* 2009;68:1290–5.
 22. Moon SJ, Ahn IE, Jung H, Yi H, Kim J, Kim Y, et al. Temporal differential effects of proinflammatory cytokines on osteoclastogenesis. *Int J Mol Med* 2013;31:769–77.
 23. Busso N, So A. Mechanisms of inflammation in gout. *Arthritis Res Ther* 2010;12:206.
 24. Sokolove J, Lepus CM. Role of inflammation in the pathogenesis of osteoarthritis: latest findings and interpretations. *Ther Adv Musculoskelet Dis* 2013;5:77–94.
 25. Pearle AD, Scanzello CR, George S, Mandl LA, DiCarlo EF, Peterson M, et al. Elevated high-sensitivity C-reactive protein levels are associated with local inflammatory findings in patients with osteoarthritis. *Osteoarthritis Cartilage* 2007;15:516–23.
 26. Yokota K, Sato K, Miyazaki T, Kitaura H, Kayama H, Miyoshi F, et al. Combination of tumor necrosis factor alpha and interleukin-6 induces mouse osteoclast-like cells with bone resorption activity both *in vitro* and *in vivo*. *Arthritis Rheumatol* 2014;66:121–9.
 27. de Hooge AS, van de Loo FA, Bennink MB, Arntz OJ, de Hooge P, van den Berg WB. Male IL-6 gene knock out mice developed more advanced osteoarthritis upon aging. *Osteoarthritis Cartilage* 2005;13:66–73.
 28. van de Loo FA, Kuiper S, van Enkevort FH, Arntz OJ, van den Berg WB. Interleukin-6 reduces cartilage destruction during experimental arthritis. A study in interleukin-6-deficient mice. *Am J Pathol* 1997;151:177–91.
 29. Kitamura H, Kawata H, Takahashi F, Higuchi Y, Furuichi T, Ohkawa H. Bone marrow neutrophilia and suppressed bone turnover in human interleukin-6 transgenic mice. A cellular relationship among hematopoietic cells, osteoblasts, and osteoclasts mediated by stromal cells in bone marrow. *Am J Pathol* 1995;147:1682–92.
 30. Gao Y, Grassi F, Ryan MR, Terauchi M, Page K, Yang X, et al. IFN-gamma stimulates osteoclast formation and bone loss *in vivo* via antigen-driven T cell activation. *J Clin Invest* 2007;117:122–32.
 31. Takayanagi H, Ogasawara K, Hida S, Chiba T, Murata S, Sato K, et al. T-cell-mediated regulation of osteoclastogenesis by signalling cross-talk between RANKL and IFN-gamma. *Nature* 2000;408:600–5.
 32. Ahmad R, El Mabrouk M, Sylvester J, Zafarullah M. Human osteoarthritic chondrocytes are impaired in matrix metalloproteinase-13 inhibition by IFN-gamma due to reduced IFN-gamma receptor levels. *Osteoarthritis Cartilage* 2009;17:1049–55.
 33. Blaine TA, Rosier RN, Puzas JE, Looney RJ, Reynolds PR, Reynolds SD, et al. Increased levels of tumor necrosis factor-alpha and interleukin-6 protein and messenger RNA in human peripheral blood monocytes due to titanium particles. *J Bone Joint Surg Am* 1996;78:1181–92.
 34. Ingham E, Green TR, Stone MH, Kowalski R, Watkins N, Fisher J. Production of TNF-alpha and bone resorbing activity by macrophages in response to different types of bone cement particles. *Biomaterials* 2000;21:1005–13.
 35. Burton L, Paget D, Binder NB, Bohner K, Nestor BJ, Sculco TP, et al. Orthopedic wear debris mediated inflammatory osteolysis is mediated in part by NALP3 inflammasome activation. *J Orthop Res* 2013;31:73–80.
 36. St Pierre CA, Chan M, Iwakura Y, Ayers DC, Kurt-Jones EA, Finberg RW. Periprosthetic osteolysis: characterizing the innate immune response to titanium wear-particles. *J Orthop Res* 2010;28:1418–24.
 37. Rakshit DS, Ly K, Sengupta TK, Nestor BJ, Sculco TP, Ivashkiv LB, et al. Wear debris inhibition of anti-osteoclastogenic signaling by interleukin-6 and interferon-gamma. Mechanistic insights and implications for periprosthetic osteolysis. *J Bone Joint Surg Am* 2006;88:788–99.
 38. Evans RW, Cheung HS, McCarty DJ. Cultured human monocytes and fibroblasts solubilize calcium phosphate crystals. *Calcif Tissue Int* 1984;36:645–50.
 39. Nicholson GC, Malakellis M, Collier FM, Cameron PU, Holloway WR, Gough TJ, et al. Induction of osteoclasts from CD14-positive human peripheral blood mononuclear cells by receptor activator of nuclear factor kappaB ligand (RANKL). *Clin Sci (Lond)* 2000;99:133–40.
 40. Kadono Y, Okada F, Perchonock C, Jang HD, Lee SY, Kim N, et al. Strength of TRAF6 signalling determines osteoclastogenesis. *EMBO Rep* 2005;6:171–6.
 41. Matsumoto M, Sudo T, Saito T, Osada H, Tsujimoto M. Involvement of p38 mitogen-activated protein kinase signaling pathway in osteoclastogenesis mediated by receptor activator of NF-kappa B ligand (RANKL). *J Biol Chem* 2000;275:31155–61.
 42. Rawlings JS, Rosler KM, Harrison DA. The JAK/STAT signaling pathway. *J Cell Sci* 2004;117:1281–3.
 43. Schroder K, Hertzog PJ, Ravasi T, Hume DA. Interferon-gamma: an overview of signals, mechanisms and functions. *J Leukoc Biol* 2004;75:163–89.
 44. You M, Yu DH, Feng GS. Shp-2 tyrosine phosphatase functions as a negative regulator of the interferon-stimulated Jak/STAT pathway. *Mol Cell Biol* 1999;19:2416–24.
 45. Schlesinger N, Thiele RG. The pathogenesis of bone erosions in gouty arthritis. *Ann Rheum Dis* 2010;69:1907–12.
 46. Yoshitake F, Itoh S, Narita H, Ishihara K, Ebisu S. Interleukin-6 directly inhibits osteoclast differentiation by suppressing receptor activator of NF-kappaB signaling pathways. *J Biol Chem* 2008;283:11535–40.
 47. Takahashi N, Mundy GR, Roodman GD. Recombinant human interferon-gamma inhibits formation of human osteoclast-like cells. *J Immunol* 1986;137:3544–9.
 48. Ohishi M, Matsumura Y, Aki D, Mashima R, Taniguchi K, Kobayashi T, et al. Suppressors of cytokine signaling-1 and -3

- regulate osteoclastogenesis in the presence of inflammatory cytokines. *J Immunol* 2005;174:3024–31.
49. Zhou Y, Mohan A, Moore DC, Lin L, Zhou FL, Cao J, et al. SHP2 regulates osteoclastogenesis by promoting preosteoclast fusion. *FASEB J* 2015;29:1635–45.
50. Laquerriere P, Grandjean-Laquerriere A, Jallot E, Balossier G, Frayssinet P, Guenounou M. Importance of hydroxyapatite particles characteristics on cytokines production by human monocytes *in vitro*. *Biomaterials* 2003;24:2739–47.